DAVID W. TAYLOR NAVAL SHIP RESEARCH AND DEVELOPMENT CENTER

Bethesda, Maryland 20084

BASIN HYDRODYNAMIC EVALUATION OF THE

8-18-F INTEGRATED TOWLINE

by

J. W. Johnston

and

H. P. Stottmeister

SHIP PERFORMANCE DEPARTMENT

June 1984

DTNSRDC/SPD 1112-01

MAJOR DTNSRDC ORGANIZATIONAL COMPONENTS

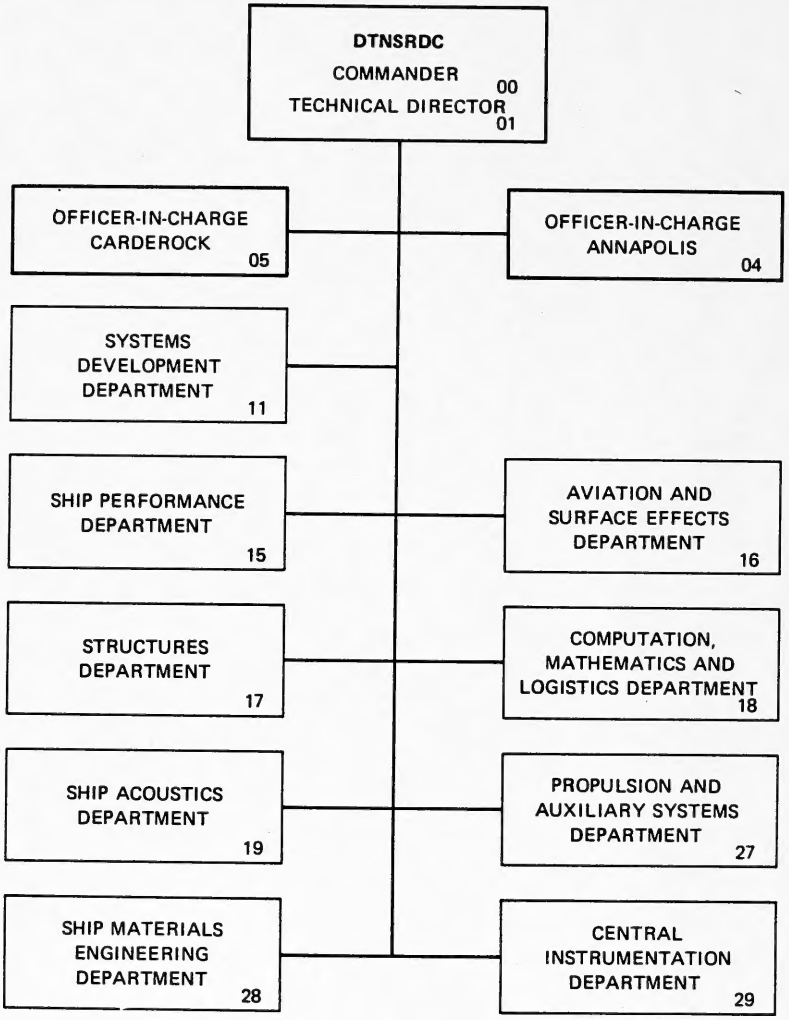

UNCLASSIFIED

SECURITY CLASSIFICATION OF THIS PAGE *(When Data Entered)*

REPORT DOCUMENTATION PAGE

READ INSTRUCTIONS BEFORE COMPLETING FORM

1. REPORT NUMBER: DTNSRDC/SPD 1112-01	2. GOVT ACCESSION NO.
3. RECIPIENT'S CATALOG NUMBER	
4. TITLE *(and Subtitle)*: BASIN HYDRODYNAMIC EVALUATION OF THE 8-18-F INTEGRATED TOWLINE	5. TYPE OF REPORT & PERIOD COVERED: Departmental
	6. PERFORMING ORG. REPORT NUMBER
7. AUTHOR(s): J. W. Johnston and H. P. Stottmeister	8. CONTRACT OR GRANT NUMBER(s)
9. PERFORMING ORGANIZATION NAME AND ADDRESS: David Taylor Naval Ship R&D Center, Code 1541, Ship Performance Department, Bethesda, Maryland 20084	10. PROGRAM ELEMENT, PROJECT, TASK AREA & WORK UNIT NUMBERS: WR - 21203, Element - 62734N, DTNSRDC WU-1-1541-076
11. CONTROLLING OFFICE NAME AND ADDRESS: Commander (548), Naval Air Systems Command, Washington, D.C. 20372	12. REPORT DATE: June 1984
	13. NUMBER OF PAGES: 42
14. MONITORING AGENCY NAME & ADDRESS *(if different from Controlling Office)*	15. SECURITY CLASS. *(of this report)*: UNCLASSIFIED
	15a. DECLASSIFICATION/DOWNGRADING SCHEDULE

16. DISTRIBUTION STATEMENT *(of this Report)*

Distribution limited to U.S. Government Agencies Only; Test and Evaluation; October 1979. Other requests for this document must be referred to David Taylor Naval Ship Research and Development Center (Code 1541), Bethesda, Maryland 20084.

17. DISTRIBUTION STATEMENT *(of the abstract entered in Block 20, if different from Report)*

18. SUPPLEMENTARY NOTES

19. KEY WORDS *(Continue on reverse side if necessary and identify by block number)*

Faired Towline
Integrated Fairing

20. ABSTRACT *(Continue on reverse side if necessary and identify by block number)*

Five integrated faired towline configurations based on a blunt nose fairing design were experimentally evaluated in the David Taylor Naval Ship Research and Development Center deep-water towing basin to determine the general towing characteristics of each configuration. Mathematical expressions of the normal drag and side force coefficients are developed from the measured data.

DD FORM 1 JAN 73 1473 EDITION OF 1 NOV 65 IS OBSOLETE
S/N 0102-014-6601

UNCLASSIFIED

SECURITY CLASSIFICATION OF THIS PAGE *(When Data Entered)*

TABLE OF CONTENTS

LIST OF FIGURES

LIST OF FIGURES (Cont'd)

LIST OF FIGURES (Cont'd)

LIST OF TABLES

THIS PAGE INTENTIONALLY LEFT BLANK.

NOTATION

A	Constant coefficient in normal drag and side force coefficient fitted functions
A_n	Coefficient of cos (n ϕ) terms in hydrodynamic loading function
A_o	Constant coefficient in hydrodynamic loading function
B	Cable buoyancy per unit lingth in a fluid
B_n	Coefficient of sin (n ϕ) terms in hydrodynamic loading function
C	Fairing generalized force coefficient
c	Fairing chord length
C_R	Fairing normal drag coefficient
C_S	Fairing side force coefficient
F	Cable hydrodynamic force component per unit length normal to a cable element in the plane defined by the cable element and the free stream direction
F_s	Cable hydrodynamic side force per unit length at the orientation of the cable that produces the maximum value
f_n, f_t, f_s	Normal, tangential and side force hydrodynamic loading functions
G	Cable hydrodynamic force component per unit length tangential to a cable element
H	Cable hydrodynamic force component per unit length normal to the plane defined by a cable element and the free stream direction
K	Constant coefficient in normal drag and side force coefficient fitted functions
R	Cable drag per unit length when the cable is normal to the free stream direction
R_n	Reynolds number based on chord length
s	Towline scope length
T	Towline tension
t	Maximum fairing thickness
V	Free-stream velocity

W_a	Towline weight per unit length in air
X	Axis of space-fixed orthogonal coordinate system positive in direction of tow (negative in free-stream direction)
Y	Axis of space-fixed orthogonal coordinate system positive to starboard
Z	Axis of space-fixed orthogonal coordinate system positive in the direction of gravity
X′, Y′, Z′	Intermediate coordinate system defined by a rotation of angle β about the X-axis
β	Towline kite angle measured from the Z-axis to the tangent of a towline element projected onto the Y-Z plane
ν	Fluid kinematic viscosity
ρ	Fluid density
ϕ	Towline angle measured from the free-stream direction (X-axis) to the tangent of a cable element

ABSTRACT

Five integrated faired towline configurations based on a blunt nose fairing design were experimentally evaluated in the David Taylor Naval Ship Research and Development Center deep-water towing basin to determine the general towing characteristics of each configuration. Mathematical expressions of the normal drag and side force coefficients are developed from the measured data.

ADMINISTRATIVE INFORMATION

The work described in this report was sponsored by the Naval Air Systems Command under Naval Coastal Systems Center WR21203 of 5 October 1981, David Taylor Naval Ship Research and Development Center (DTNSRDC) Work Unit 1-1541-076.

INTRODUCTION

The David Taylor Naval Ship Research and Development Center (DTNSRDC) has been tasked by the Naval Air Systems Command (NAVAIR) to develop towlines for helicopter towed sonar systems with high speed and deep depth requirements exceeding the practical capabilities that can be provided with bare, ribbon or sectional faired towcables. To achieve the speed/depth requirements with a towline length that can be handled in the space limitations of a mine-countermeasures (MCM) configured helicopter, the towline should have a high tensile strength load-carrying element, a small bending radius, and minimum drag. Integrated towline concepts have demonstrated the necessary high-strength, low-drag characteristics, but in many cases have demonstrated susceptibility to hydrodynamic/mechanical instabilities and shape asymmetries which result in excessive towline kiting.

Integrated towlines developed previously were designed using established symmetric airfoil shapes such as the NACA 0020 and NACA 63A022 profiles. A modified version of the NACA 0020 towline was evaluated at sea and demonstrated acceptable towing characteristics[1].* Figure 1 presents a cross-sectional view of the NACA 0020 towline, showing the typical features of the integrated towline design which include a fiberglass strength member, an elastomeric afterbody fairing, electrical conductors and a Dacron® cloth skin. Although this design provides a very high axial strength-to-size towline, it also produces a high

* References are listed on page 39.

® Trade name of DuPont de Nemours, Inc.

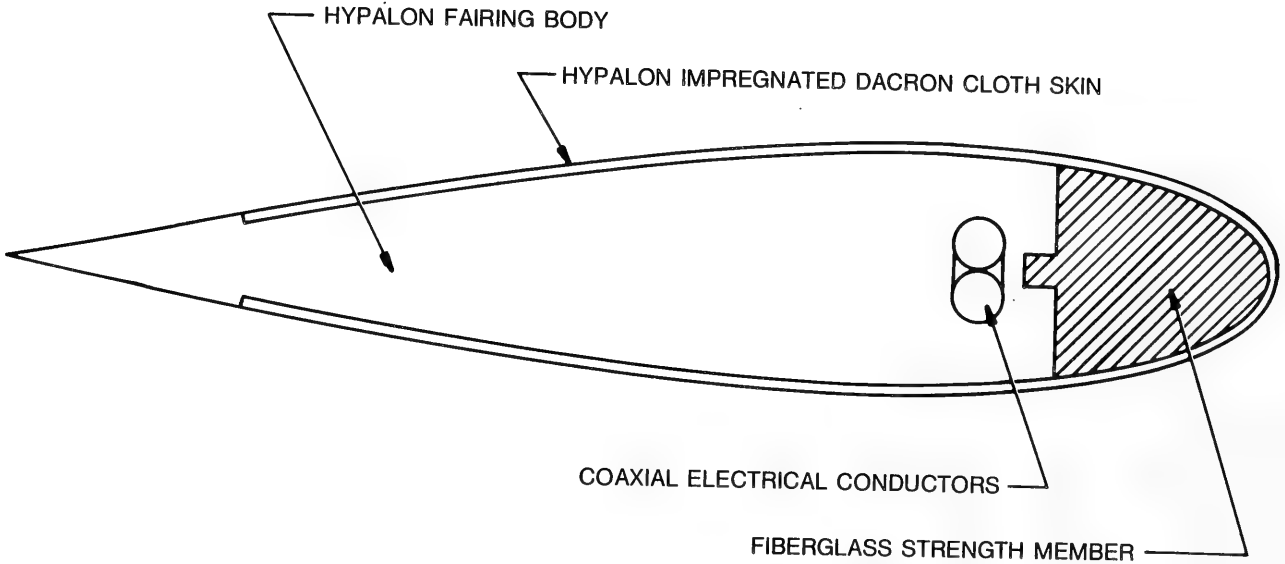

Figure 1 - Illustration of the NACA 0020 Towline Design

bending stiffness which requires storage drum and sheave diameters to be approximately 2.5 times larger than those required for conventional cables of the same maximum thickness (diameter).

Consequently, the NACA 0020 towline could not be wrapped around a diameter smaller than 1.5 m (5 ft) without damaging the electrical conductors or exceeding the allowable stresses in the fiberglass strength member. The minimum bending radius governs to a large extent the size of the handling equipment, which for the NACA 0020 towline design exceeds the space limitations of the MCM helicopter. Therefore, to utilize the integrated towline concept for helicopter MCM operations, a new towline design was required.

DTNSRDC developed a new fairing shape, designated 8-18-F, based upon results of basin model evaluations[2], sonar system power and data transmission requirements, towing tension, and space limitations of the MCM helicopter. A 19-foot length of experimental 8-18-F towline was obtained for basin evaluations to examine its susceptibility to kiting and to obtain hydrodynamic drag and side force characteristics.

This report includes a description of the experimental integrated towline configurations, outlines the experiment, instrumentation, and experimental procedures used to collect data, and provides the results of the evaluation including graphical presentations of the normal drag and side force coefficients as a function of Reynolds number and kite angle as a function of towing speed for several towline configurations. Basin and at-sea data obtained for the NACA 0020 integrated towline with truncation are included for comparative purposes.

DESCRIPTION OF THE EXPERIMENTAL INTEGRATED TOWLINES

A cross-sectional view of the experimental 8-18-F integrated towline, designated Configuration A-1 in this report, is presented in Figure 2, and general physical characteristics are given in Table 1. The 8-18-F towline materials and general construction are similar to those of the NACA 0020 towline, except that the strength member was designed with a blunt nose (leading edge) and a recessed trailing edge. This shape accommodates the required power and data transmission leads, consisting of six AWG number 17 solid copper electrical conductors and four 50 m optic fiber cores. Each of the electrical conductors and optic fibers is coated with a ruggedizing material consisting of an S-glass/epoxy resin. The leads are separated into two bundles of three copper conductors and two optic

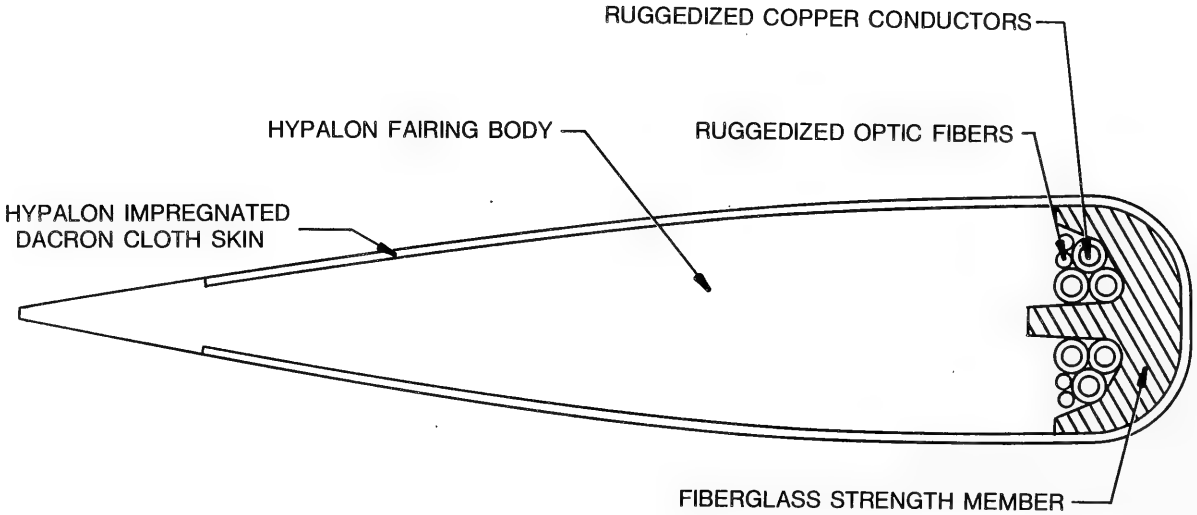

Figure 2 - Illustration of the 8-18-F (Configuration A-1) Towline Design

TABLE 1 - GENERAL PHYSICAL CHARACTERISTICS OF THE 8-18-F (CONFIGURATION A-1) INTEGRATED TOWLINE DESIGN

	8-18-F	
Overall Characteristics		
Section shape[2]		
Chord, mm (in.)	63.50	(2.50)
Maximum thickness, mm (in.)	12.70	(0.50)
Weight in air, N/m (lb/ft)	8.552	(0.586)
Weight in sea-water, N/m (lb/ft)	2.877	(0.193)
Weight in fresh-water, N/m (lb/ft)	2.977	(0.204)
Strength Member		
(Material - 80 percent parallel fiber "S" glass/20 percent epoxy matrix)		
Cross-sectional area, mm^2 ($in.^2$)	57.161	(0.0886)
Breaking strength, kN (lb)	93.413	(21000)
Fairing		
(Main body material - Dupont Hypalon®)		
(Skin material - Dupont Hypalon impregnated Dacron® cloth D-400)		
Skin thickness, mm (in.)	0.51	(0.02)

fibers which are bonded into recesses as shown in Figure 2. The portion of the towline strength member separating the two conductor bundles is 1.6-mm (1/16-in.) wide and extends 1.6 mm (1/16 in.) into the Hypalon® afterbody and acts as a key to prevent lateral displacement of the afterbody relative to the strength member.

Figure 3 illustrates the modified 8-18-F towline configurations, designated B-1, C-1, C-2 and C-3, that also were evaluated in the towing basin. The trailing edges of towlines B-1 and C-1 were truncated using an alternating bevel geometry. The B-1 geometry was produced by beveling the trailing edge of the A-1 towline at a 45-degree angle, alternating the bevel from side to side at 0.3-m (12-in.) intervals. Configuration C-1 was produced by increasing the bevel depth of the B-1 fairing. The B-1 and C-1 geometries reduce the original A-1 towline chord by an average of approximately 9 and 16 percent, respectively.

Figure 3 - Illustrations of Modified 8-18-F Towline Designs

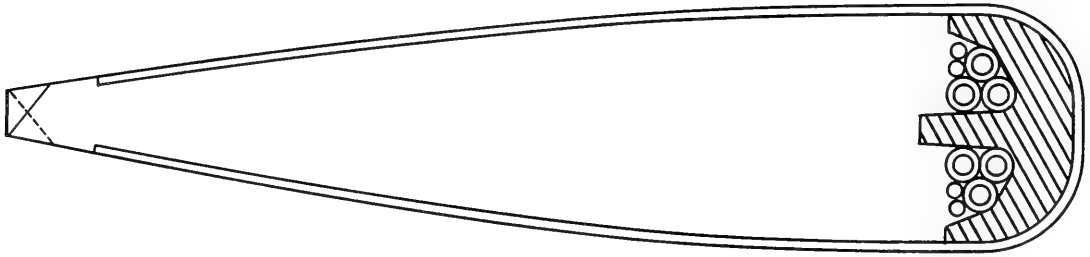

Figure 3a - Configuration B-1 (9 Percent Truncation)

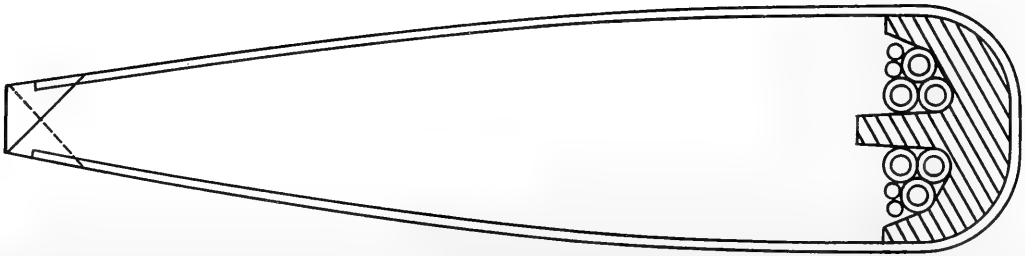

Figure 3b - Configuration C-1 (16 Percent Truncation)

Figure 3 (Continued)

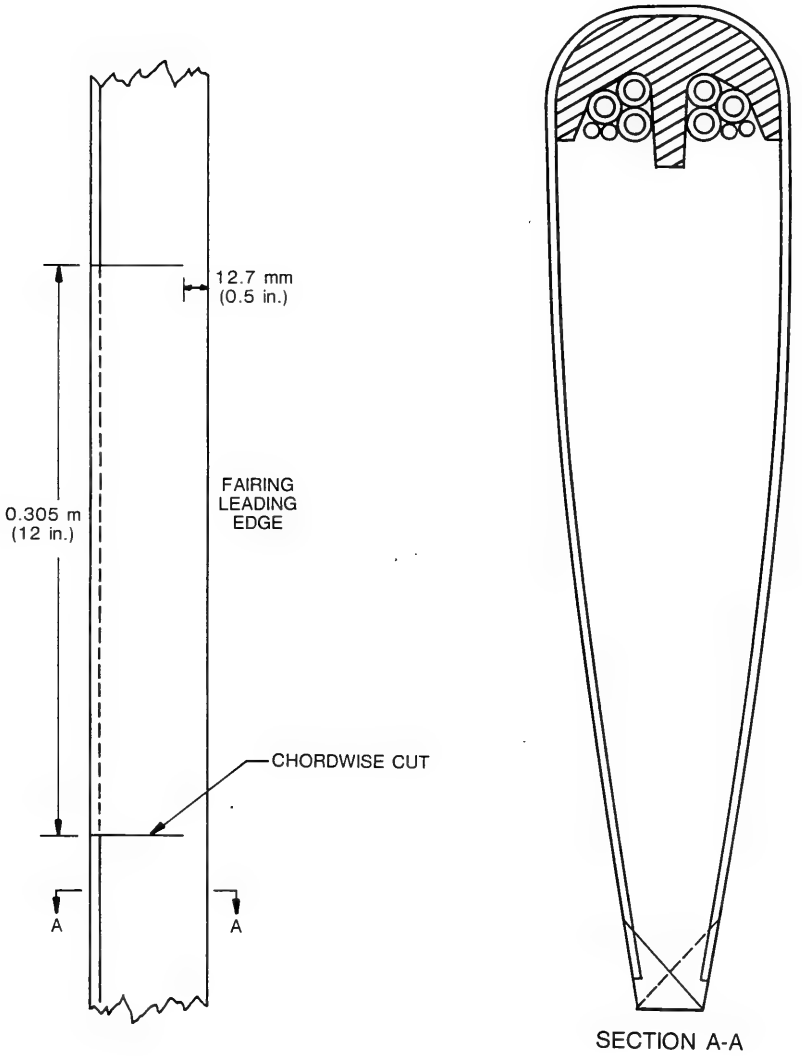

Figure 3c - Configuration C-2 (16 Percent Truncation with One Chordwise Cut per Foot of Span)

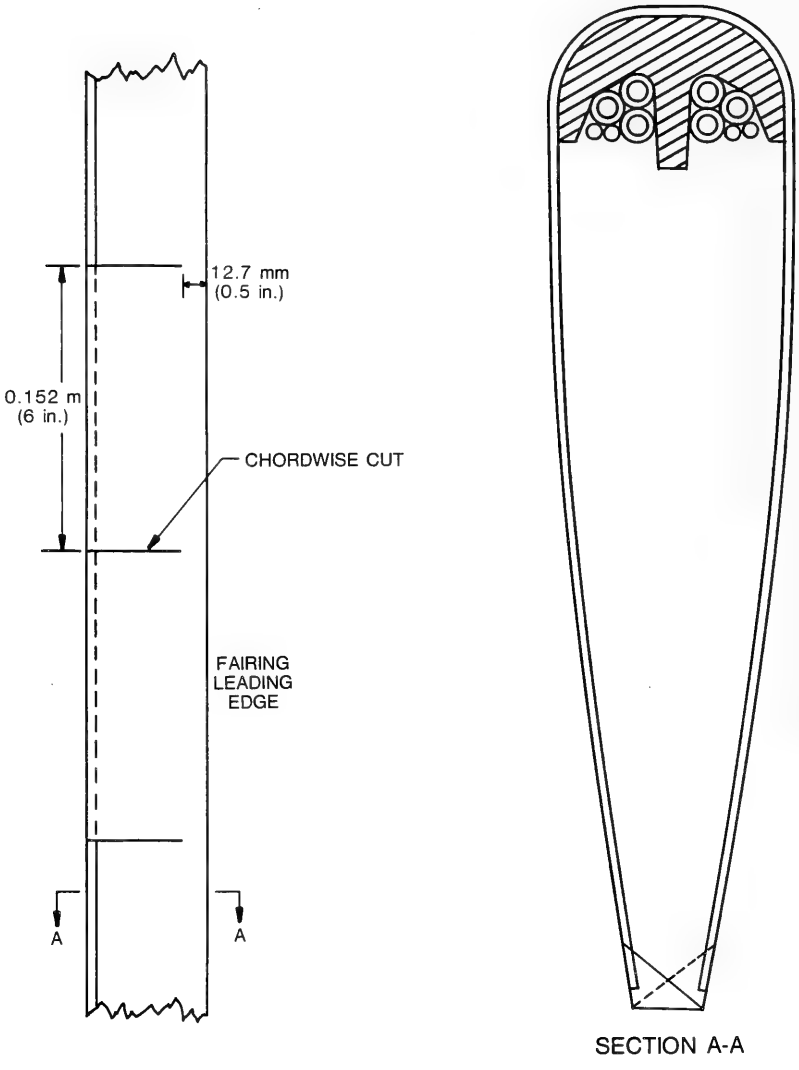

Figure 3d - Configuration C-3 (16 Percent Truncation With Two Chordwise Cuts per Foot of Span)

The C-2 configuration was produced by making chordwise cuts to within 12.7 mm (1/2 in.) of the C-1 towline leading edge at 0.3-m (12-in.) spanwise intervals along the towline. The C-3 configuration was produced by doubling the number of the chordwise cuts from 0.3-m (12-in.) intervals to 0.15-m (6-in.) intervals along the towline length.

For purposes of evaluation, a 5.8-m (19-ft) length of configuration A-1 towline was used. The B-1, C-1, C-2 and C-3 configurations were obtained by successive modifications of configuration A-1 during the basin evaluation. A 5.8-m (19-ft) length of NACA 0020 integrated towline (14 percent truncation with 45 degree alternating bevels) was also evaluated for comparison with the 8-18-F configurations.

EXPERIMENTAL EVALUATIONS

Experiments to determine the hydrodynamic characteristics of the 8-18-F towline design were performed in the DTNSRDC deep-water towing basin using the general towing arrangement shown in Figure 4. The coordinate system, equipment, instrumentation, and procedures used during this evaluation are described below.

COORDINATE AND FORCE SYSTEM

The differential equations describing the three-dimensional static configuration and tension of a cable in a uniform stream are derived from the equilibrium of external forces acting on an element of the cable. A free-body diagram showing a segment of cable of elemental length ds acted upon by hydrodynamic, hydrostatic, gravitational, and tension forces is illustrated in Figure 5. The (X, Y, Z) coordinate system shown is a right-hand, orthogonal system fixed in space with the X-axis positive in the direction of tow (or negative in the free-stream direction) and the Z-axis positive in the direction of gravity.

The equations are conveniently derived for an orthogonal coordinate system fixed to the cable. In Figure 5, the hydrodynamic force has been resolved into components Fds, Gds, and Hds where F is the force component per unit length normal to the cable in the plane defined by the cable element and the free-stream direction, G is the force component per unit length tangential to the cable, and H is the (side) force component per unit length normal to the plane defined by the cable element and the free-stream direction. The cable-fixed coordinate system

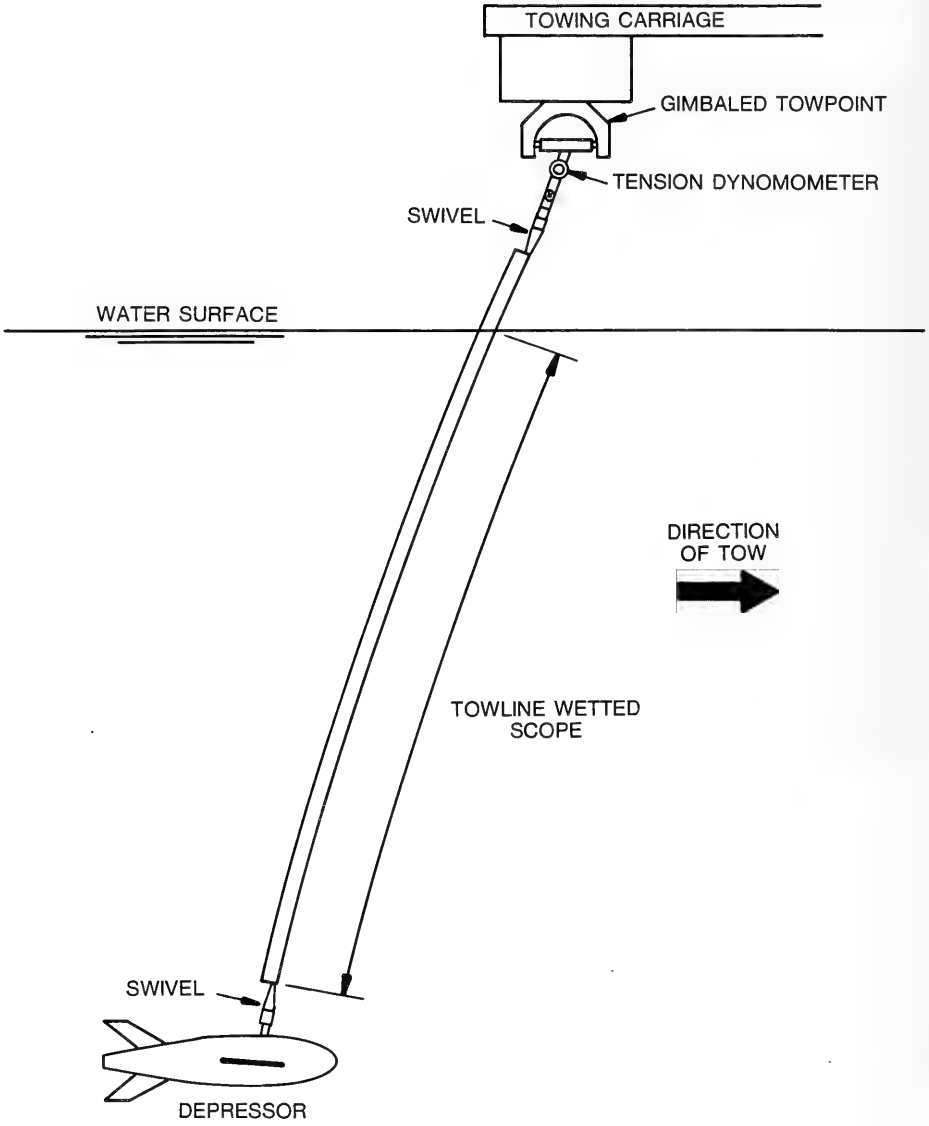

Figure 4 - General Towing Arrangement

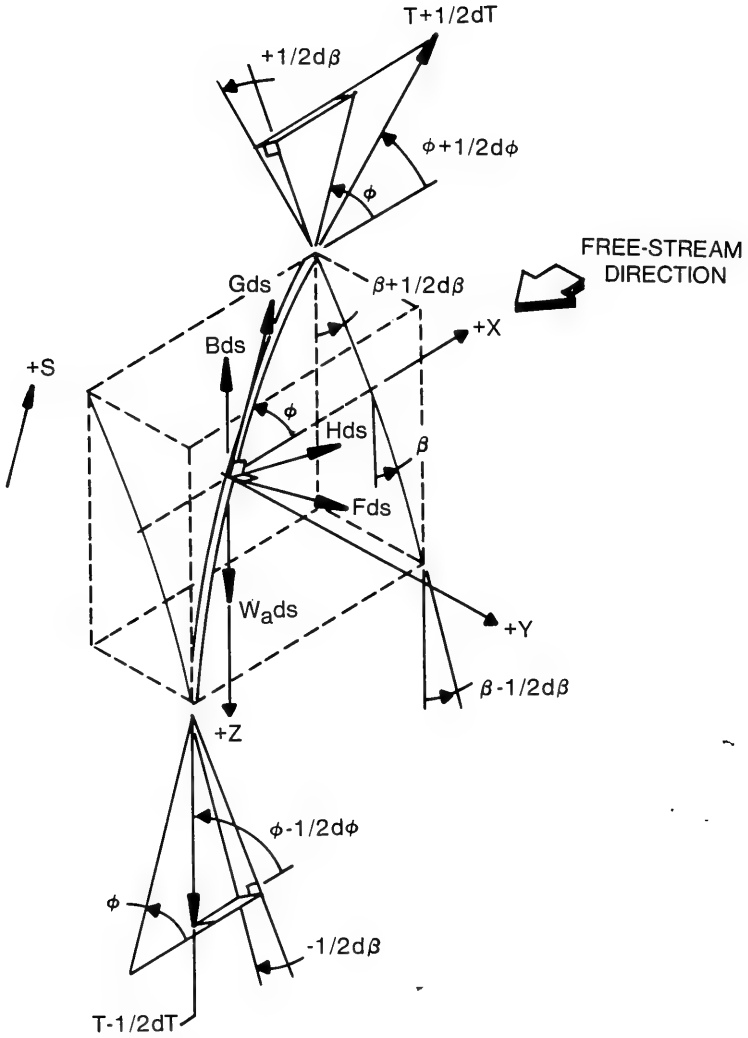

Figure 5 - Definition of Cable Coordinates and Forces Acting on a Segment of Towline of Element Length ds

defined by the directions of F, G, and H may be obtained by first rotating the spatial system by an angle β about the X-axis and then rotating the resulting intermediate (X′, Y′, Z′) coordinate system by an angle ϕ about the Y′-axis. In towed systems nomenclature, the angles β and ϕ generally are referred to as the kite angle and the cable angle, respectively. Since the orientation of the cable changes in space, the angles β and ϕ are functions of cable length s.

EQUIPMENT

The depressor used during the evaluation was a DTMB Mark 1 knotmeter[3] which was modified by replacing the standard knotmeter wing with a larger wing and adapting a towpoint that allowed limited pitch, roll, and yaw freedom relative to the towline. Top and side views of the knotmeter with the larger wing installed are shown in Figure 6. The new knotmeter towpoint, illustrated in Figure 7, allows the knotmeter approximately 18 degrees of port and starboard roll freedom, 20 degrees of pitch freedom, and 30 degrees of port and starboard yaw freedom.

At the towing carriage, the towline was attached to a gimbaled towpoint through a swivel and tension dynamometer arrangement as shown in Figure 8. The gimbaled towpoint permitted port and starboard kite angles from 0 to 60 degrees and cable angles from 90 to 40 degrees. Both kite and cable angle measurements were provided by rotary potentiometers attached to the gimbaled towpoint and to the kite and cable angle pivots through anti-backlash gear sets. Both gear sets were arranged so that the potentiometer shaft rotation was three times that of the corresponding kite or cable angle pivot. The swivel located immediately above the towline socket provided the towline 360 degrees of yaw freedom. Tow speed was limited to 9.28 m/s (18 knots), which is the maximum speed of the deep-water basin towing carriage with this towing load.

INSTRUMENTATION

Instrumentation located at the depressor consisted of a $\pm$20-degree pendulous potentiometer which provided depressor roll angle measurement with an overall accuracy of $\pm$0.5 degree.

Instrumentation and analog recording equipment located at the towing carriage provided measurements of towing tension, kite angle, cable angle, carriage speed and records of all measured data. The tension dynomometer used during the evaluation had a 2.7-kN (600-lb) load capacity and provided towing tension

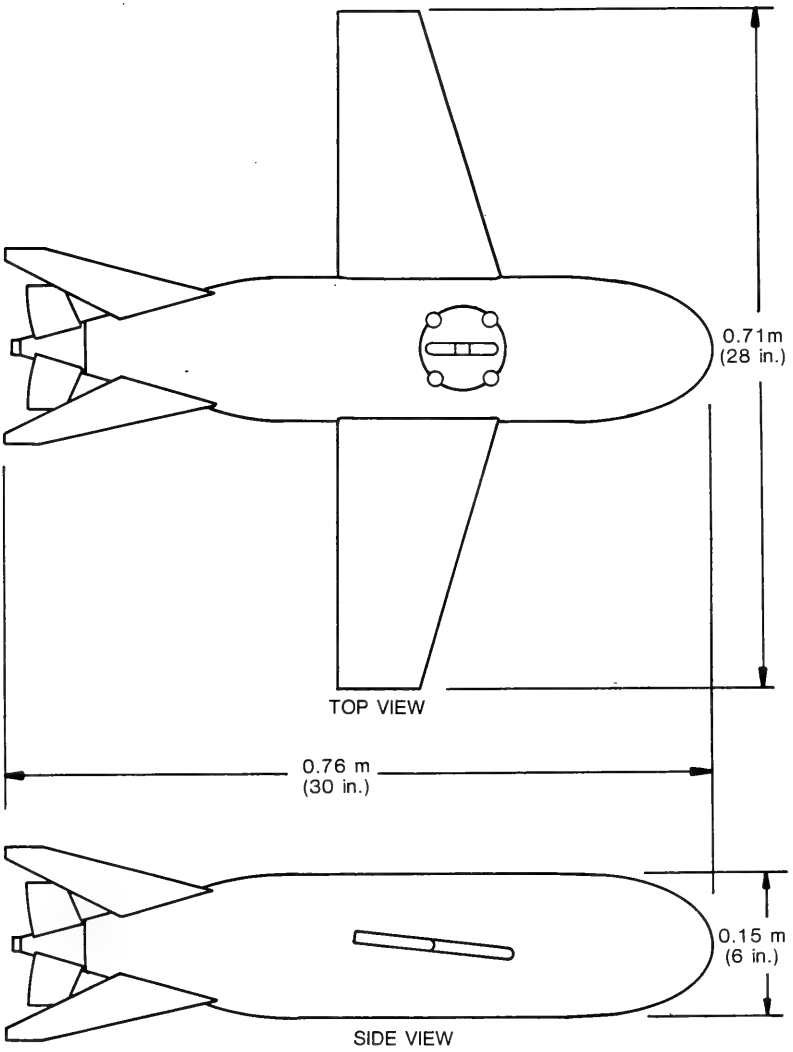

Figure 6 - Modified DTMB Mark 1 Knotmeter

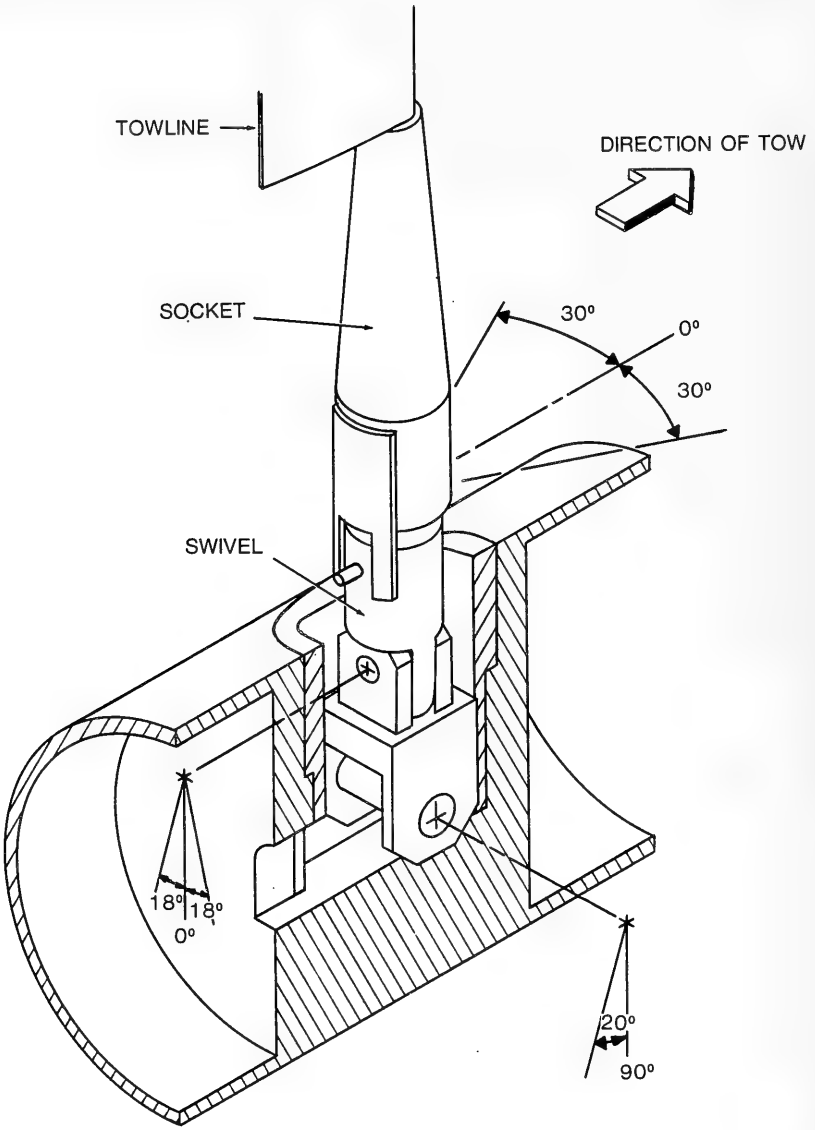

Figure 7 - Illustration of Modified Knotmeter Towpoint

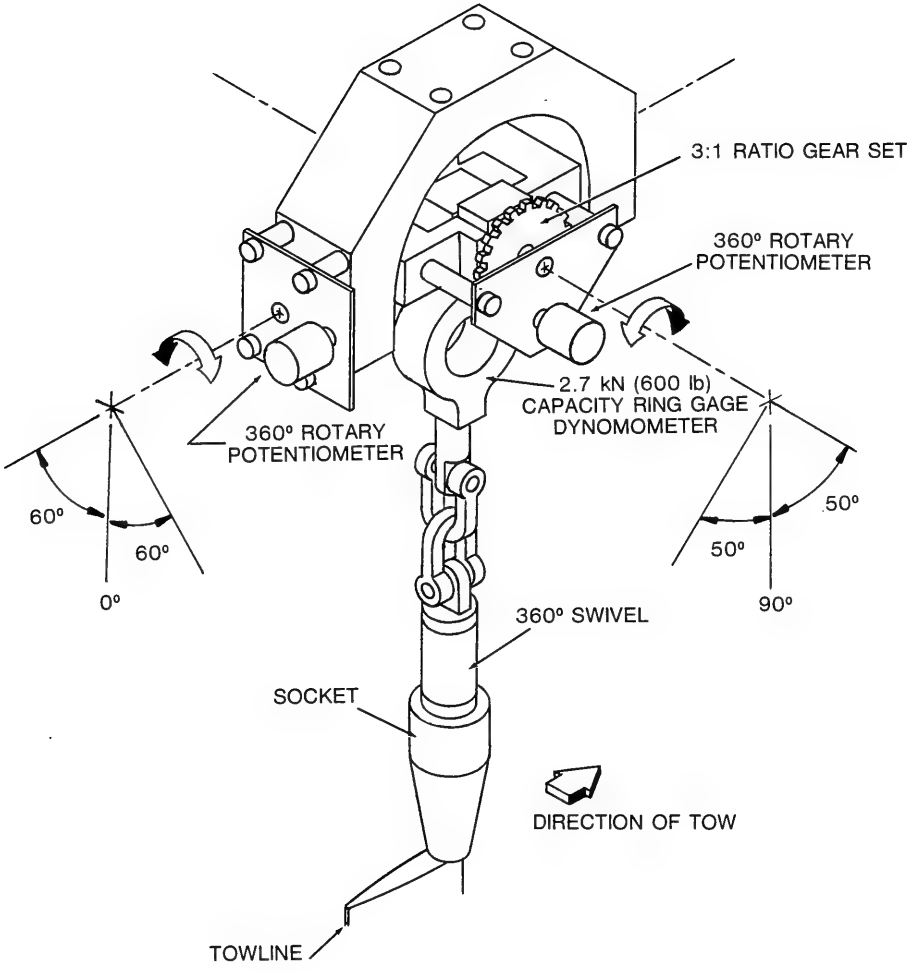

Figure 8 - Illustration of Gimbaled Towpoint

measurements with an overall accuracy of ±13.3 N (±3 lb). Two 360-degree rotary potentiometers attached to the gimbaled towpoint (Figure 8) provided measurements of towline kite and cable angle. These potentiometers, in conjuction with the three-to-one ratio gear sets, provided angle measurements of ±60 degrees with an overall accuracy of ±0.3 degree. Carriage speed measurements were supplied from a magnetic pickup located on the towing carriage. This speed measurement technique has an overall accuracy of ±.05 m/s (±0.1 knot). An eight-channel strip-chart recorder was used for readout and recording of all measured data.

PROCEDURES

Towing performance was examined for wetted scopes of 3.7 m (12.3 ft) and 5.7 m (18.8 ft) for towline configurations A-1, B-1, C-1, C-2 and the 14 percent bevel truncated NACA 0020 towline through a speed range from 1.03 m/s (2.0 knots) to 9.26 m/s (18 knots). Configuration C-3 was examined through the speed range at a scope of 5.7 m (18.8 ft). Depressor roll angle, towing tension, kite angle, cable angle, towline wetted scope, tow speed and visual observations of the general towing performance were recorded during each experimental run.

DISCUSSION OF RESULTS

All of the towline configurations towed in an acceptable manner (i.e., stably and with small kiting angles). Figures 9 through 11 present the average corrected kite angle for each towline configuration towed at the 5.7-m (18.8-ft) scope length as a function of tow speed. The corrected kite angles were determined by subtracting the measured depressor roll angle from the kite angle measured at the gimbaled towpoint for each speed. This corrects for the component of towline kite angle induced by the roll angle of the depressor. Averaged data for all measured parameters recorded during the evaluation of each towline configuration are listed in Table 2.

As shown in Figures 9 through 11, all of the towline configurations demonstrated increasing kite angle with increasing speed up to approximately 8 knots. Above this speed the kite angle generally remained at a constant value. This effect is not a towline characteristic, but is a result of the depressor selected for the evaluation. Since the depressor used was a negatively buoyant lifting body, the in-water weight tends to dominate the hydrodynamic force at speeds below approximately 4.12 m/s (8 knots). At speeds above 4.12 m/s

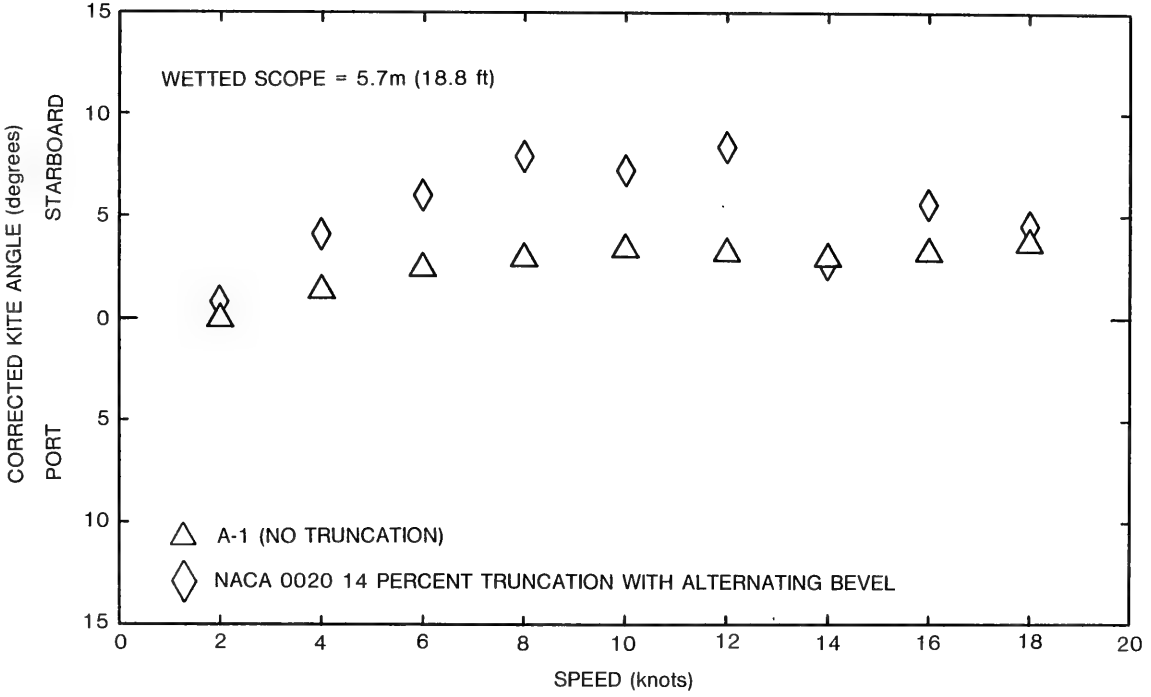

Figure 9 - Corrected Kite Angle Versus Speed for Towline Configuration A-1 and the NACA 0020 Towline with a 14 Percent Bevel Truncation

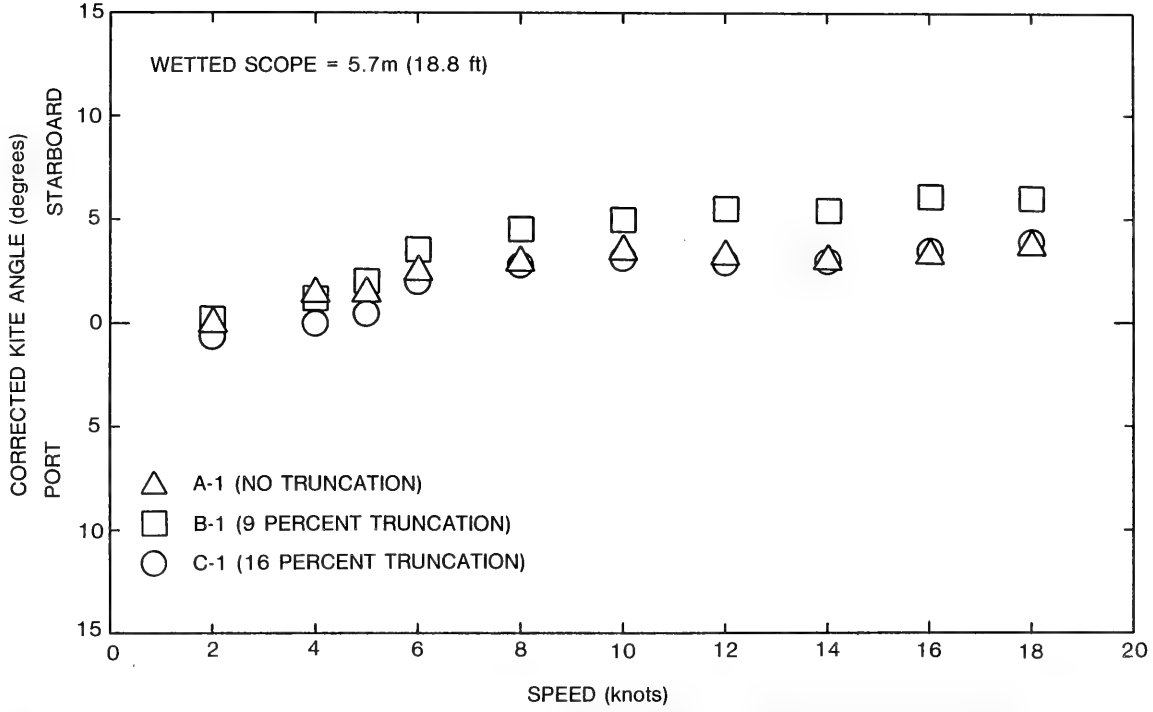

Figure 10 - Corrected Kite Angle Versus Speed
for Towline Configurations A-1, B-1, and C-1

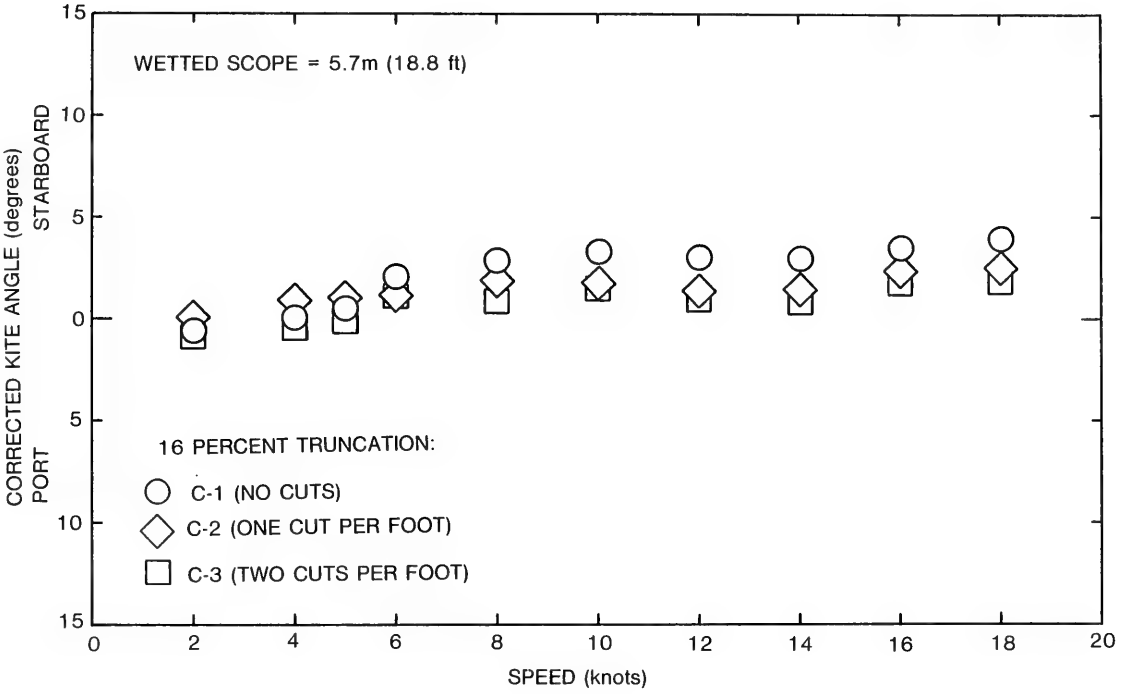

Figure 11 - Corrected Kite Angle Versus Speed for Towline Configurations C-1, C-2, and C-3

TABLE 2 - INTEGRATED TOWLINE BASIN EVALUATION DATA

Wetted Scope m (ft)	Tow Speed knots	Towing Tension kN (lb)	Cable Angle degrees	Kite Angle degrees	Depressor Roll Angle degrees	Corrected Kite Angle degrees
3.75 (12.3)	2	0.55 (124)	89.5	+ 0.3	- 0.5	+ 0.8
	4	0.54 (121)	86.3	+ 0.5	- 0.3	+ 0.8
	6	0.66 (148)	82.1	+ 2.1	0.0	+ 2.1
	8	0.84 (189)	77.8	+ 4.3	+ 1.8	+ 2.5
	10	1.08 (242)	75.5	+ 4.5	+ 2.8	+ 1.7
	12	1.34 (302)	73.4	+ 4.5	+ 2.4	+ 2.1
	14	1.66 (374)	72.6	+ 6.1	+ 4.4	+ 1.7
	16	2.04 (458)	72.1	+ 2.4	+ 0.1	+ 2.3
3.75 (12.3)	18	2.46 (553)	71.1	+ 2.4	- 0.3	+ 2.7
5.72 (18.8)	2	0.55 (123)	87.5	+ 0.3	- 0.3	+ 0.6
	4	0.54 (122)	83.5	+ 1.8	- 0.3	+ 2.1
	6	0.66 (148)	78.1	+ 2.5	- 0.1	+ 2.6
	8	0.84 (189)	74.3	+ 4.1	+ 1.0	+ 3.1
	10	1.07 (240)	71.8	+ 5.8	+ 2.8	+ 3.0
	12	1.33 (300)	70.3	+ 6.5	+ 3.3	+ 3.2
	14	1.66 (374)	69.5	+ 6.9	+ 4.3	+ 2.6
	16	2.02 (454)	68.4	+ 3.4	- 0.1	+ 3.5
5.72 (18.8)	18	2.45 (550)	68.3	+ 3.6	- 0.1	+ 3.7
	CONFIGURATION B-1					
3.75 (12.3)	2	0.55 (124)	87.5	+ 0.3	0.0	+ 0.3
	4	0.54 (122)	84.5	+ 1.5	0.0	+ 1.5
	6	0.65 (147)	79.8	+ 2.6	0.0	+ 2.6
	8	0.82 (184)	76.1	+ 4.0	- 0.3	+ 4.3
	10	1.04 (234)	73.3	+ 5.3	+ 1.3	+ 4.0
	12	1.31 (294)	71.5	+ 7.8	+ 3.0	+ 4.8
	14	1.61 (361)	70.0	+ 9.4	+ 5.0	+ 4.4
	16	1.96 (440)	69.5	+ 6.0	+ 1.3	+ 4.7
3.75 (12.3)	18	2.39 (538)	68.8	+ 6.0	+ 1.0	+ 5.0
5.73 (18.8)	2	0.54 (122)	87.0	+ 0.3	0.0	+ 0.3
	4	0.54 (121)	83.0	+ 1.3	0.0	+ 1.3
	6	0.64 (144)	77.8	+ 3.5	0.0	+ 3.5
	8	0.81 (183)	73.3	+ 4.5	- 0.1	+ 4.4
	10	1.04 (234)	70.0	+ 7.6	+ 2.5	+ 5.1
	12	1.32 (296)	68.4	+ 8.1	+ 2.6	+ 5.5
	14	1.61 (361)	66.8	+10.3	+ 4.9	+ 5.4
	16	1.97 (442)	66.3	+ 7.6	+ 1.5	+ 6.1
5.73 (18.8)	18	2.39 (538)	66.9	+ 7.5	+ 1.5	+ 6.0

TABLE 2 - CONTINUED

Wetted Scope m (ft)	Tow Speed knots	Towing Tension kN (lb)	Cable Angle degrees	Kite Angle degrees	Depressor Roll Angle degrees	Corrected Kite Angle degrees
	CONFIGURATION C-1					
3.75 (12.3)	2	0.55 (123)	87.0	+ 0.4	+ 0.3	+ 0.1
	4	0.54 (121)	84.0	+ 1.3	+ 0.3	+ 1.0
	6	0.64 (144)	79.5	+ 2.5	+ 0.3	+ 2.2
	8	0.82 (184)	76.0	+ 4.1	+ 1.5	+ 2.6
	10	1.04 (233)	72.9	+ 5.5	+ 2.5	+ 3.0
	12	1.30 (292)	70.3	+ 6.3	+ 2.8	+ 3.5
	14	1.59 (357)	69.1	+ 7.3	+ 3.9	+ 3.4
	16	1.91 (429)	67.9	+ 4.4	0.0	+ 4.4
3.75 (12.3)	18	--- ---	---	---	---	---
5.73 (18.8)	2	0.54 (122)	87.0	0.0	+ 0.6	- 0.6
	4	0.54 (121)	82.1	+ 0.8	+ 0.8	0.0
	6	0.65 (146)	76.5	+ 2.4	+ 0.4	+ 2.0
	8	0.82 (185)	72.1	+ 3.1	+ 0.3	+ 2.8
	10	1.03 (231)	68.9	+ 3.9	+ 0.6	+ 3.3
	12	1.30 (292)	66.5	+ 7.4	+ 4.4	+ 3.0
	14	1.58 (356)	65.0	+ 8.1	+ 5.0	+ 3.1
	16	1.95 (439)	64.0	+ 7.8	+ 4.3	+ 3.5
5.73 (18.8)	18	2.37 (532)	63.4	+ 9.1	+ 5.3	+ 3.8
	CONFIGURATION C-2					
3.75 (12.3)	2	0.55 (124)	88.0	+ 0.3	+ 0.4	- 0.1
	4	0.54 (122)	84.0	+ 0.9	+ 0.4	+ 0.5
	6	0.65 (146)	78.9	+ 1.6	+ 0.5	+ 1.1
	8	0.83 (186)	74.8	+ 2.1	+ 0.5	+ 1.6
	10	1.04 (234)	72.0	+ 2.5	+ 0.5	+ 2.0
	12	1.31 (294)	70.0	+ 6.0	+ 4.3	+ 1.7
	14	1.60 (360)	68.5	+ 7.8	+ 6.1	+ 1.7
	16	1.95 (438)	67.6	+ 6.6	+ 4.4	+ 2.2
3.75 (12.3)	18	2.38 (534)	67.4	+ 7.9	+ 4.9	+ 3.0
5.73 (18.8)	2	0.54 (122)	87.0	+ 0.4	+ 0.3	+ 0.1
	4	0.54 (121)	82.3	+ 1.1	+ 0.3	+ 0.8
	6	0.64 (145)	76.3	+ 1.5	+ 0.3	+ 1.2
	8	0.81 (182)	71.9	+ 2.2	+ 0.4	+ 1.8
	10	1.04 (234)	68.8	+ 3.0	+ 1.3	+ 1.7
	12	1.30 (293)	66.4	+ 5.6	+ 4.3	+ 1.3
	14	1.59 (358)	64.9	+ 7.9	+ 6.5	+ 1.4
	16	1.95 (438)	63.9	+ 6.8	+ 4.4	+ 2.4
5.73 (18.8)	18	2.38 (535)	63.1	+ 7.9	+ 5.4	+ 2.5

TABLE 2 - CONTINUED

Wetted Scope m (ft)	Tow Speed knots	Towing Tension kN (lb)	Cable Angle degrees	Kite Angle degrees	Depressor Roll Angle degrees	Depressor Kite Angle degrees
	CONFIGURATION C-3					
5.73 (18.8)	2	0.54 (122)	86.0	- 0.1	+ 0.7	- 0.8
	4	0.53 (119)	81.5	+ 0.3	+ 0.7	- 0.4
	6	0.64 (144)	77.1	+ 1.6	+ 0.5	+ 1.1
	8	0.82 (184)	72.8	+ 2.0	+ 0.6	+ 1.4
	10	1.03 (231)	69.5	+ 1.8	+ 0.3	+ 1.5
	12	1.28 (288)	67.5	+ 5.6	+ 4.6	+ 1.0
	14	1.60 (359)	66.0	+ 7.4	+ 6.5	+ 0.9
	16	1.95 (438)	64.6	+ 6.3	+ 4.5	+ 1.8
5.73 (18.8)	18	2.37 (533)	64.0	+ 7.5	+ 5.8	+ 1.7
	NACA 0020 (14 PERCENT ALTERNATING BEVEL TRUNCATION)					
3.75 (12.3)	2	0.55 (123)	88.0	+ 0.3	0.0	+ 0.3
	4	0.54 (121)	85.1	0.0	- 0.1	+ 0.1
	6	0.63 (142)	81.5	+ 2.5	- 0.1	+ 2.6
	8	0.81 (182)	78.0	+ 3.5	+ 0.9	+ 2.6
	10	1.04 (233)	75.5	+ 7.3	+ 2.4	+ 4.9
	12	1.30 (292)	73.5	+ 8.9	+ 2.8	+ 6.1
	14	1.58 (355)	72.1	+ 3.0	+ 4.9	- 1.9
	16	1.94 (436)	71.1	+ 2.8	+ 1.2	+ 1.6
3.75 (12.3)	18	2.31 (520)	70.5	+ 0.3	+ 0.8	- 0.5
5.73 (18.8)	2	0.54 (121)	87.5	+ 0.9	0.0	+ 0.9
	4	0.52 (117)	84.0	+ 4.1	- 0.1	+ 4.2
	6	0.64 (143)	80.5	+ 6.0	- 0.1	+ 6.1
	8	0.80 (183)	76.5	+ 8.6	+ 0.9	+ 7.7
	10	1.03 (231)	73.3	+10.1	+ 2.4	+ 7.7
	12	1.29 (290)	71.1	+11.3	+ 2.8	+ 8.5
	14	1.57 (353)	69.5	+ 7.5	+ 4.9	+ 2.6
	16	1.93 (433)	68.5	+ 6.8	+ 1.2	+ 5.6
5.73 (18.8)	18	2.31 (520)	68.0	+ 5.5	+ 0.8	+ 4.7

(8 knots), the hydrodynamic force becomes dominant and the system (towline and depressor) steady-state force variations become essentially proportional to the square of tow speed.

As shown in Figure 9 configuration A-1 demonstrated approximately 3 degrees of kite at speeds above 4.12 m/s (8 knots). The truncated 0020 towline (shown in this figure for comparative purposes) demonstrated 7 degrees of kite from 4.12 m/s (8 knots) to 6.19 m/s (12 knots) and at speeds above 7.22 m/s (14 knots) demonstrated approximately 4-1/2 degrees of kite. The reduction in the kite angle between 6.19 and 7.22 m/s (12 and 14 knots) is believed to be attributable to the hydrodynamic forces and moments above 6.19 m/s (12 knots) overcoming those produced by the fairing structural instability.

The kite angles for configurations B-1 and C-1 are compared to A-1 in Figure 10. B-1 demonstrated approximately 5-1/2 degrees of kite at speeds above 4.12 m/s (8 knots), which is approximately 1 degree more kite than configuration A-1, while C-1 demonstrated approximately 4 degrees of kite, which essentially is the same degree of kite demonstrated by A-1. The slightly larger kite angle measured with the B-1 configuration is believed to be caused by asymmetries introduced during the truncation process.

Figure 11 presents the kite angle for configurations C-2 and C-3 compared to C-1. The C-2 and C-3 configurations demonstrated a trend of reduced kiting with increasing frequency of chordwise cuts. Above 4.12 m/s (8 knots) the C-2 configuration demonstrated 3 degrees of kite and approximately 1-1/2 degrees of kite for C-3 while C-1 demonstrated 4 degrees of kite.

DETERMINATION OF TOWLINE HYDRODYNAMIC COEFFICIENTS

The three-dimensional equilibrium configuration and forces of a towline-body system were solved using a computer program[4] which required the following hydrodynamic input parameters: the tension vector at some point on the towline, the towline drag and side force coefficients and the towline drag and side force loading functions. The towline drag components, normal and tangential, are assumed to be the product of a drag per unit length, which is a function of Reynolds number R_n and a loading function which is a function of cable angle ϕ. Using this convention, the normal force per unit length F and the tangential force per unit length G are of the following form:

$$F(R_n, \phi) = -R(R_n) \cdot f_n(\phi) \quad (1)$$

$$G(R_n, \phi) = -R(R_n) \cdot f_t(\phi) \quad (2)$$

where R is the towline drag per unit length when the towline is normal to the direction of tow ($R = 1/2 \quad C_R \, tV^2$),

R_n is the Reynolds number ($R_n = V c/\nu$),

is the fluid density,

C_R is the towline normal drag coefficient expressed as a function of Reynolds number,

t is the towline maximum thickness,

c is the fairing chord,

V is the free-stream flow velocity,

ν is the fluid kinematic viscosity, and

f_n, f_t are the normal and tangential loading functions, respectively.

The negative (-) signs in the equations for $F(R_n, \phi)$ and $G(R_n, \phi)$ above appear since the towline drag is in the negative (-) X-direction as defined in Figure 5.

For purposes of evaluation, the side force component per unit length is assumed to be composed of a product of a maximum side force that is dependent only upon Reynolds number R_n and a loading function that is dependent only upon cable angle ϕ as follows:

$$H(R_n, \phi) = F_s(R_n) \cdot f_s(\phi) \quad (3)$$

where F_s is the towline side force per unit length at the cable angle that produces the maximum value ($F_s = 1/2 \, \rho \, C_s \, t \, V^2$); which for the integrated towline occurs when the towline is normal ($\phi = 90$ degrees) to the direction of tow.

C_s is the towline side force coefficient expressed as a function of Reynolds number, and

f_s is the hydrodynamic side loading function.

However, in actuality the fairing side force is a function of many other variables some of which include angle of attack, camber, and twist along the towline length. Since the individual effects of all the variables contributing to the side force are currently indeterminate by evaluation or analysis, the expression for the side force stated above will only provide an average side-force coefficient for the towline segment evaluated. Utilizing the coefficients so determined to predict the performance of other towline segments of the same design implies that the magnitudes and distributions of the fairing variables causing the side force are identical. This implication may not be the case.

To obtain an estimate of the normal drag and side-loading coefficients the form of the loading functions must be known or assumed. For this purpose, previously determined normal and tangential loading functions for the 8-18-F integrated fairing shape[2] and the NACA 0020 shape[1] were used. The side-loading function for both the 8-18-F and NACA 0020 shapes was defined[5] as:

$$f_s(\phi) = \sin^2 \phi = 0.5 - 0.5 \cos(2\phi) \qquad (4)$$

The loading functions for all of the blunt nose fairing configurations were assumed to be those developed for the 8-18-F fairing. These loading functions and the NACA 0020 loading functions are shown in Figure 12 and 13, respectively. The mathematical expressions for the loading functions are given in Table 3.

Normal drag coefficients were determined by a regression analysis using the three-dimensional computer model program. For each towline configuration and speed run, average tension and angle measured at the 3.7-m (12.3-ft) scope position were used as starting conditions and the force coefficients (C_R and C_S) were varied until an acceptable agreement of predicted-to-average measured values at the 5.7-m (18.8-ft) scope position were obtained.

Side-force coefficients were determined using an analysis technique similar to that used to obtain the normal drag coefficients. To determine the average value of the side-force coefficient for each full towline length, the parameters measured at the 5.8-m (18.8-ft) scope position were used as the starting conditions in conjunction with the value of C_R determined as described above, and the value of C_S was varied until the depressor predicted roll angle agreed with the measured value.

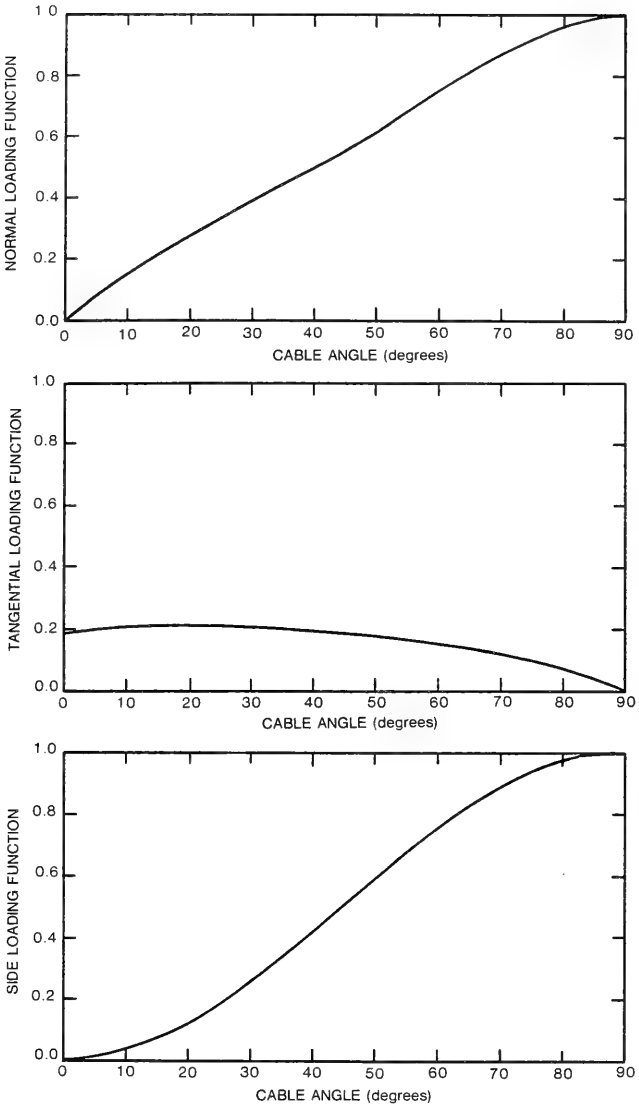

Figure 12 - Loading Functions for the NACA 0020 - 14 Percent Alternating Bevel Truncation Integrated Towline Versus Cable Angle

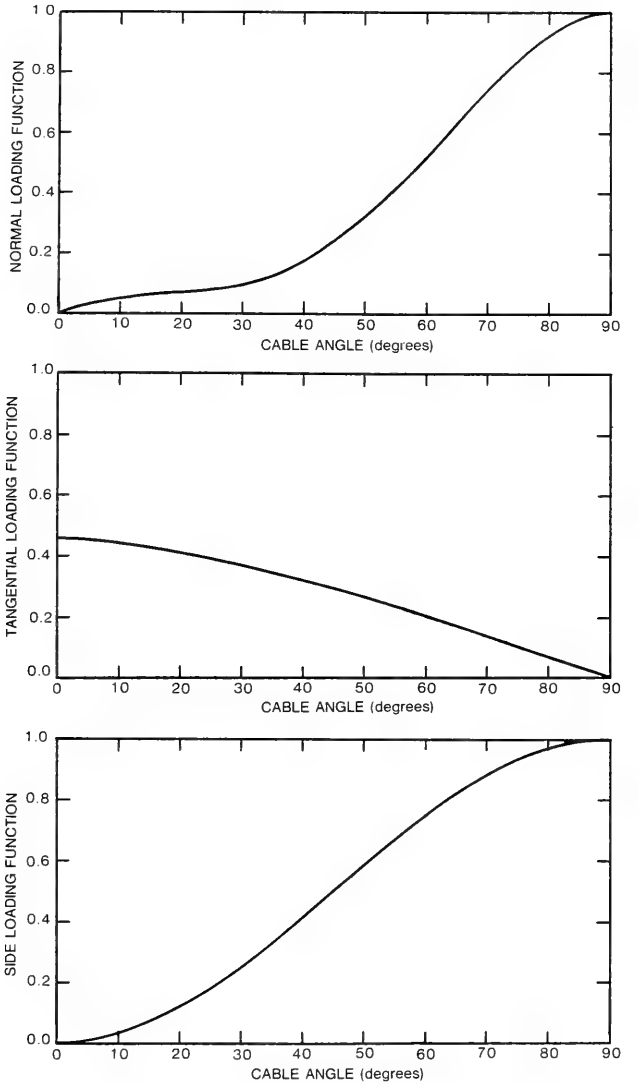

Figure 13 - Loading Functions for the 8-18-F Integrated Towline Versus Cable Angle

TABLE 3 - HYDRODYNAMIC LOADING FUNCTION COEFFICIENTS

Towline Configuration	Loading Function	Coefficients $f(\phi) = A_o + A_1 \cos \phi + B_1 \sin \phi + A_2 \cos 2\phi + B_2 \sin 2\phi$				
		A_o	A_1	B_1	A_2	B_2
NACA 0020 14 Percent Alternating Bevel Truncated	Normal	-1.852	1.833	2.871	0.019	-0.917
	Tangential	-0.80888	1.04888	075713	-0.05171	-0.28586
	Side	0.500	0	0	-0.500	0
8-18-F	Normal	-4.102	4.330	4.874	-0.228	-2.165
	Tangential	0.0776	0.3828	-0.0776	0	0
	Side	0.500	0	0	-0.500	0

Mathematical expressions for the normal drag coefficient for fairing configurations A-1, B-1, C-1, C-2 and the NACA 0020 shape, and the side force coefficient for configurations A-1, B-1, C-1, and C-2 were determined by fitting the coefficients based on measured data with an equation having the general form:

$$C = A + K/R_n \tag{5}$$

where A and K are constants determined by least-squares curve fitting.

The values of A and K that provide the best fit to each of the towline configuration's normal drag and side fore coefficients as a function of Reynolds number are presented in Table 4. The mathematical relationships presented in this table are compared to the normal drag and side force coefficients calculated from the average basin data in Figures 14 through 18.

DISCUSSION OF HYDRODYNAMIC COEFFICIENTS

The force coefficients presented in Figure 14 indicate that configuration A-1 has a normal drag coefficient that varies from approximately 0.37 to 0.17 and a side-force coefficient that varies from approximately 0.09 to 0.05 at Reynolds numbers from 2×10^5 to 6×10^5, respectively. The coefficients determined for configurations B-1 and C-1 are presented in Figures 15 and 16. By comparing the force coefficients for these configurations to those for the A-1 configuration, the effects of increasing the percentage of alternating bevel chordwise truncation may be examined. The B-1 configuration, which had a 9-percent truncation, demonstrated an average reduction of approximately 15 percent in the normal drag coefficient. The C-1 configuration, which had a 16-percent bevel truncation, demonstrated an increased normal drag coefficient of approximately 19 percent at a Reynolds number of 4.5×10^5, but as the Reynolds number decreased the normal drag coefficient approached the value for the A-1 configuration until at a Reynolds number of 2.2×10^5 the values of C_R were essentially the same for the C-1 and A-1 configurations. Although there may exist a relationship of C_R as a function of percentage alternating bevel chordwise truncation, the limited number of samples evaluated in this report do not define such a relationship and at best indicate that there is little effect on C_R for alternating bevel truncations up to chordwise truncations of 16 percent.

TABLE 4 - FITTED NORMAL DRAG AND SIDE FORCE COEFFICIENTS EQUATION CONSTANTS

Towline Configuration	Reynolds Number Range x 10^{-5}	Constants			
		$C_R = A + K/R_n$		$C_S = A + K/R_n$	
		A	K	A	K
A-1	2.7 - 6.0	0.0698	59603.9	0.0269	11680.7
B-1	2.4 - 5.5	0.0783	43570.6	0.0654	10323.7
C-1	2.2 - 4.5	0.1550	38867.2	0.0285	8759.5
C-2	2.2 - 4.5	0.2506	-1324.9	0.0218	3426.6
NACA 0020 14 Percent Alt. Bevel Truncation	2.2 - 5.0	0.1321	-1196.5	----	----

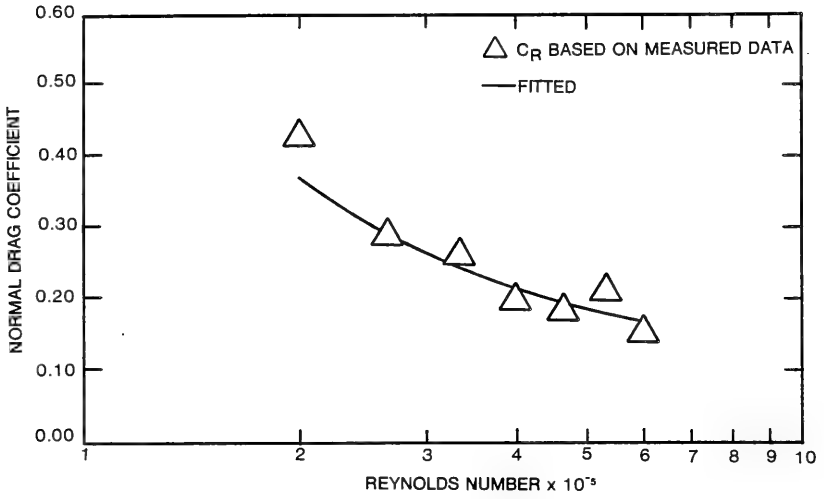

Figure 14a - Normal Drag Coefficient

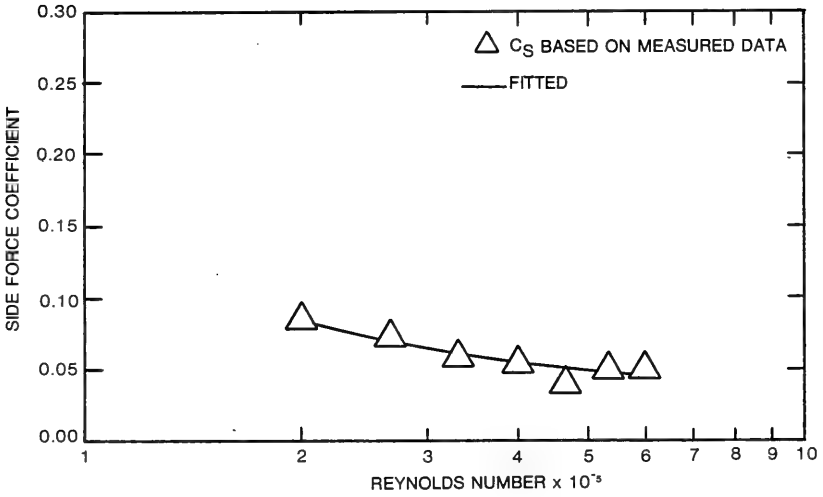

Figure 14b - Side Force Coefficient

Figure 14 - Normal Drag and Side Force Coefficients as a Function of Reynolds Number for Towline Configuration A-1

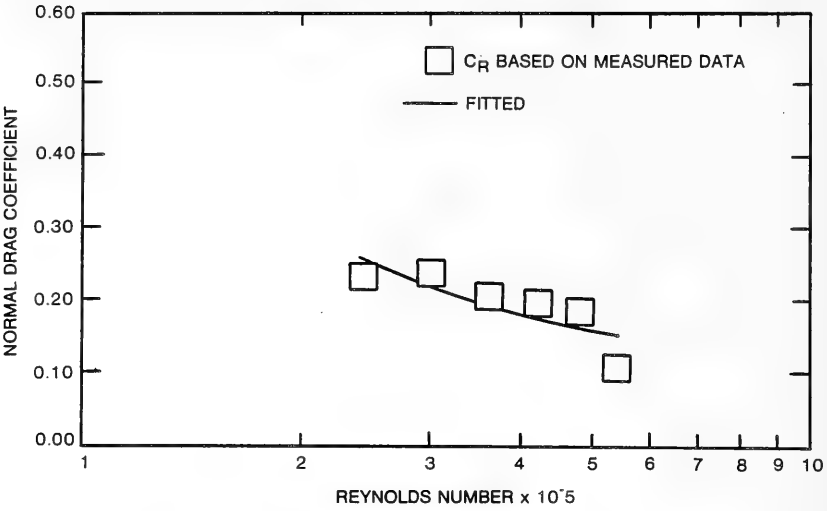

Figure 15a - Normal Drag Coefficient

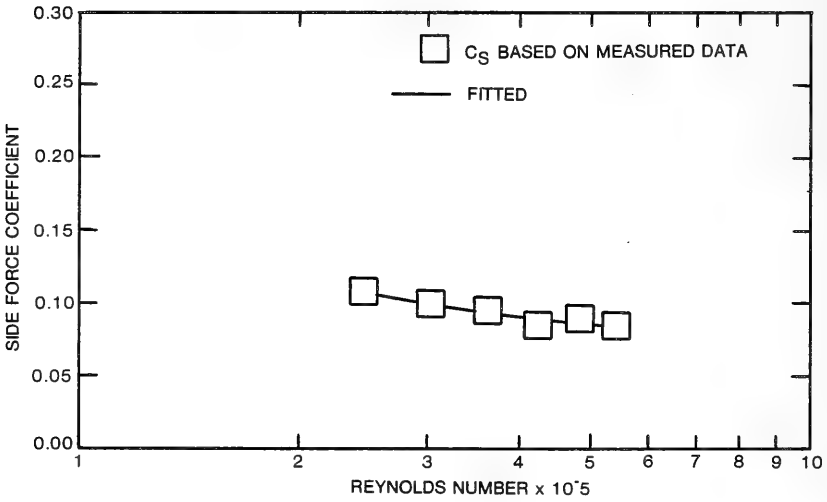

Figure 15b - Side Force Coefficient

Figure 15 - Normal Drag and Side Force Coefficients as a Function of Reynolds Number for Towline Configuration B-1

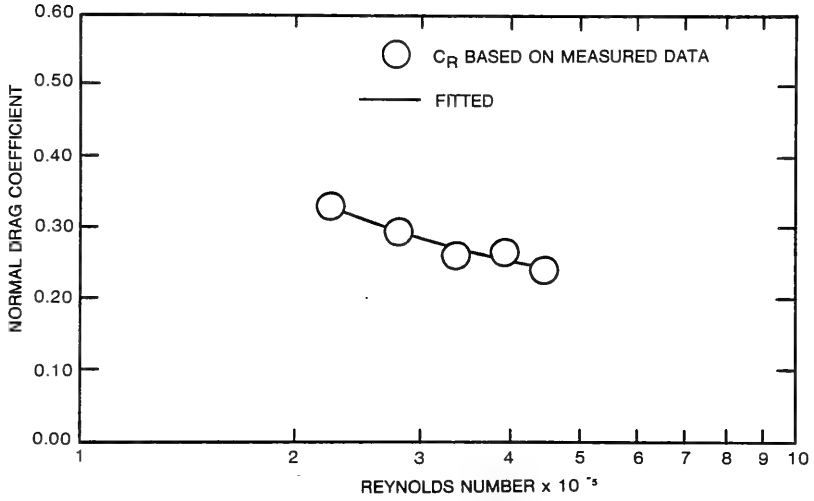

Figure 16a - Normal Drag Coefficient

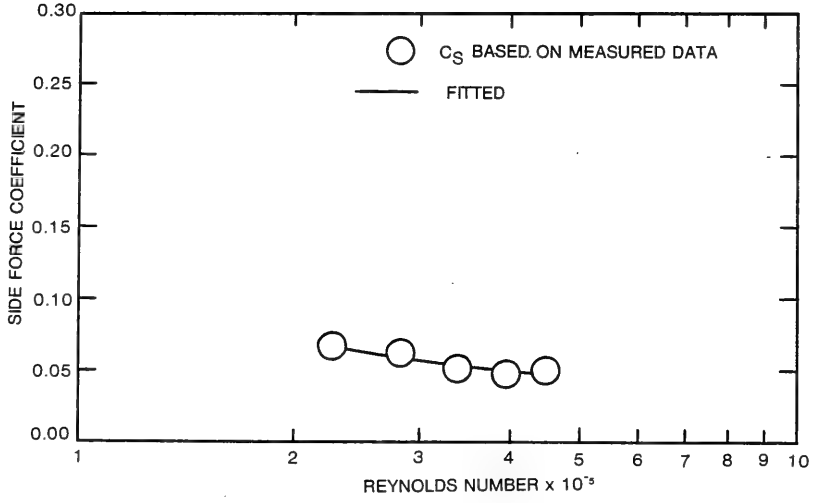

Figure 16b - Side Force Coefficient

Figure 16 - Normal Drag and Side Force Coefficients as a Function of Reynolds Number for Towline Configuration C-1

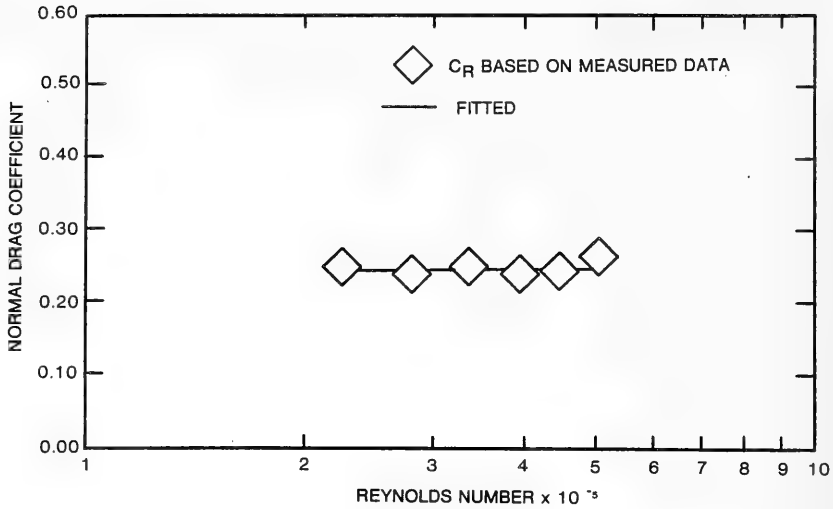

Figure 17a - Normal Drag Coefficient

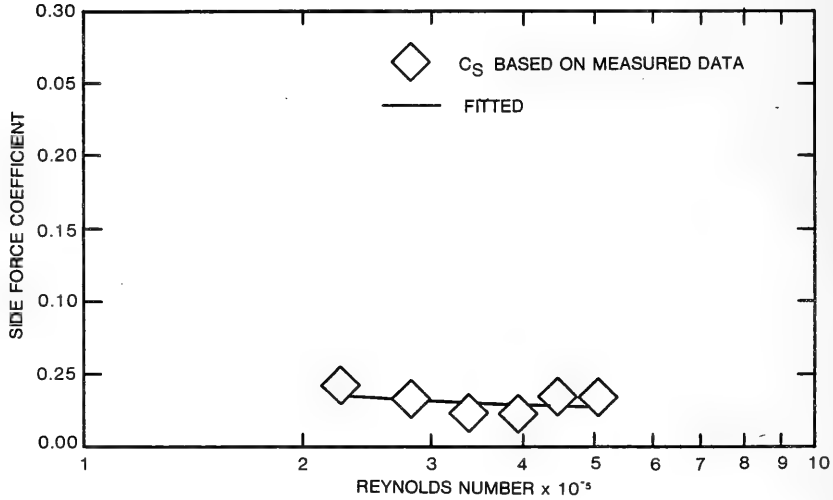

Figure 17b - Side Force Coefficient

Figure 17 - Normal Drag and Side Force Coefficients as a Function of Reynolds Number for Towline Configuration C-2

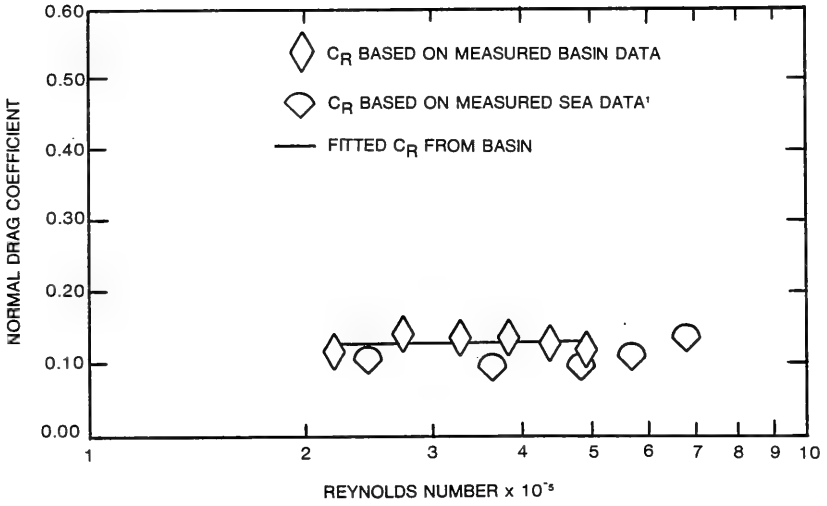

Figure 18a - Normal Drag Coefficient

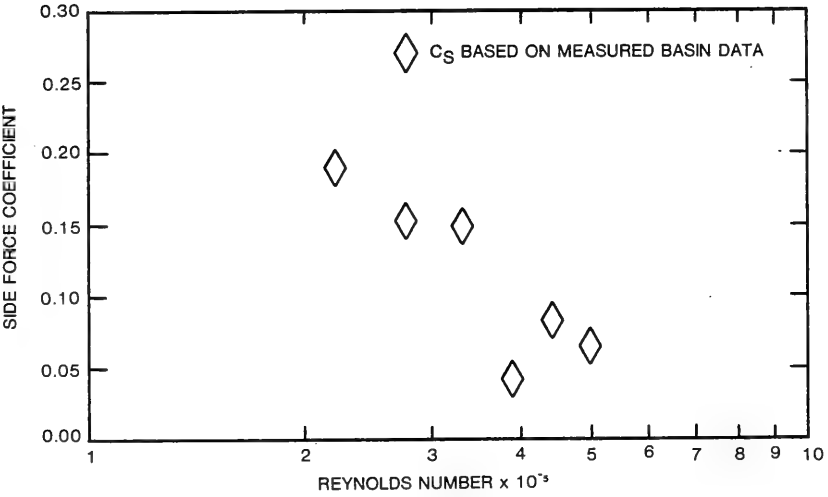

Figure 18b - Side Force Coefficient

Figure 18 - Normal Drag and Side Force Coefficients as a Function of Reynolds Number for the NACA 0020 Towline with a 14 Percent Alternating Bevel Truncation

The side-force coefficients for the B-1 configuration demonstrated an average increase of approximately 60 percent when compared to C_S determined for the A-1 configuration, while the C-1 configuration demonstrated an average reduction of approximately 12 percent. Although a large variation in side-force coefficient is shown for these configurations, these may have been the result of asymmetries introduced by the truncation process. Therefore, no distrinct trends for the side-force coefficient as a function of percentage alternating bevel chordwise truncation are discernible from the coefficients presented.

The effects of the chordwise cuts may be examined by comparing the force coefficients determined for configurations C-1 and C-2. The C-1 configuration demonstrated a variation in C_R from approximately 0.33 to 0.24 at Reynolds numbers from 2.2×10^5 to 4.5×10^5, respectively. Configuration C-2 for the same Reynolds number range as C-1 demonstrated a nearly constant value for C_R of 0.25, being essentially equal to configuration C-1 at Reynolds numbers above 3.3×10^5.

The C-1 configuration demonstrated a C_S that varied from 0.068 to 0.048 at Reynolds numbers from 2.2×10^5 to 4.5×10^5, respectively. For the C-2 configuration over the same Reynolds number range the side-force coefficient had a value approximately 73 percent lower than the C-1 configuration. Based upon this result and the actual kite angle measurements presented in a preceding section of this report for the C-1, C-2 and C-3 configurations, there is signficant evidence suggesting a trend of reduced kite for an increasing frequency of chordwise cuts. The mechanism by which the chordwise cuts reduce the kiting is not explicitly known, but is believed to be related to the reduced strain these cuts provide in the fairing trailing edge when the fairing is bent to the shape of the catenary.

Figure 18 presents the force coefficients developed for the NACA 0020 shape. The normal drag coefficients determined from the basin data are compared to the coefficients determined from at-sea data. As can be seen in Figure 18a, the C_R values from the basin data agree well with those determined from the at-sea data over the Reynolds number range of 2.2 to 5.0×10^5. The values for C_S determined from the basin data are presented in Figure 18b. Basin data only is shown since at-sea values of C_S are not available for comparison. As shown in this figure, the values of C_S demonstrate a large reduction with increasing Reynolds number. This reduction is believed to be attributable to the hydrodynamic forces and moments overcoming those produced by the fairing structural instability as Reynolds number is increased.

The mathematical expressions for the force coefficients determined for configuration A-1 are used in the Appendix to predict the kiting performance of towlines of greater length for selected speeds and depressor forces. Configuration A-1 was selected for the predictions since this configuration demonstrated a relatively low side-force coefficient and did not introduce the structural uncertainties associated with the towlines incorporating chordwise cuts. Although the calculated kiting performance may have limited quantitative value due to the imposition of assumptions required when extending these mathematical expressions to longer towline lengths, the predictions do provide a qualitative representation of the influence of cable scope, tow speed and depressor force on towline kite angle at the towing platform for a given towline configuration. In general, these calculations indicate that increasing the towline scope for a constant tow speed and depressor configuration or increasing tow speed for a constant towline scope and depressor configuration increases the kite angle at the towing platform. However, for each tow speed there appears to be a maximum value of kite angle at the towing platform that all scope lengths approach. This maximum value occurs at a discrete value of depressor force (typically low depressor force) for each scope. Variations of the depressor force above or below the force that produces this maximum kite angle will decrease the kite angle at the towing platform.

The calculations in the Appendix also indicate that, for a selected maximum allowable kite angle at the towing platform of 30 degrees, towline lengths of configuration A-1 approaching 457 m (1500 ft) could be towed at speeds up to 15.46 m/s (30 knots) provided the correct depressor force is selected. However, using these calculations as towline performance predictions for specific lengths of towline must be viewed with some degree of caution due to the assumptions associated with the mathematical expression for C_S.

CONCLUSIONS

Based on the results of the basin experiments of the integrated towline configurations, the following conclusions are made:

1. A blunt nose integrated towline can be designed to tow in a satisfactory manner. For the 8-18-F towline evaluated in this report, acceptable kiting behavior is indicated by the low side-force coefficient of approximately 0.05. The degree of kiting, however, will be influenced by such factors as depressor tension, speed, scope and variation of asymmetries. Similarly, relatively low towline drag is indicated by the normal drag coefficients which varied from approximately 0.30 to 0.15 at Reynolds numbers from 2×10^5 to 6×10^5, respectively.

2. Alternating bevel truncation has little effect on the kiting characteristics and the normal drag coefficient configurations of the blunt nose towline investigated in this report.

3. Chordwise cuts tend to reduce towline kite with little effect on the normal drag coefficient, but may increase the towline tangential drag. However, reliability associated with these cuts has not been demonstrated.

RECOMMENDATIONS

The following is recommended:

1. Longer lengths of the blunt nose towline (based upon the 8-18-F geometry) should be evaluated at-sea to verify the 8-18-F loading functions, normal drag and side-force coefficients, and hydrodynamic stability determined during basin evaluations.

2. A series of towline samples based on the 8-18-F shape with systematic variations of cross-sectional dimensions and material properties should be evaluated to determine the interactive effects of hydrodynamic and structural scaling on towline performance.

3. If chordwise cuts are implemented to reduce towline kite, the reliability of the towline should be investigated.

REFERENCES

1. Johnston, J. W., "At-Sea Evaluation of Four Modified NACA 0020 Integrated Faired Towline Designs," DTNSRDC/SPD 0920-01 (October 1979).

2. Stottmeister, H. P., "Experimental Evaluation of Several Section Shapes for Integrated Faired Towline Design," DTNSRDC/SPD 0966-01 (January 1981).

3. Springston, G. B., Jr., "The DTMB Mark 1 Knotmeter," David Taylor Model Basin Report 1944 (December 1964).

4. Knutson, R., "BASIC Desktop Computer Program for the Three-Dimensional Static Configuration of an Extensible Flexible Cable in a Uniform Stream," DTNSRDC/Research and Development Report (to be published).

5. Perkins, C. D. and R. E. Hage, "Airplane Performance Stability and Control," John Wiley and Sons, Inc., New York (1950), pp. 101-103.

THIS PAGE INTENTIONALLY LEFT BLANK

APPENDIX

CALCULATED KITING BEHAVIOR OF CONFIGURATION A-1 AT SELECTED TOW SPEEDS, TOWLINE SCOPES AND DEPRESSOR CONFIGURATIONS

Basin performance data for the towline configuration A-1 sample length provided the information necessary to develop mathematical expressions for the normal drag and side force coefficients given below:

$$C_R = 0.0698 + 59603.9/R_n \quad (6)$$

$$C_S = 0.0269 + 11680.7/R_n \quad (7)$$

These mathematical relationships in conjunction with the drag and side force loading functions, the physical characteristics of the towline, and the computer program for determining the three-dimensional equilibrium configuration of a towline-body system were used to calculate the towline configuration for selected towline scopes, tow speeds and depressor tension vectors. The resulting calculated towline catenaries can be used to examine the influence of these selected parameters on towline kite angle at the towing platform.

PROCEDURES

Calculations of the towline configuration were carried out by systematic variations of towline scope and depressor tension over a range from 91 m (300 ft) to 610 m (2000 ft) and 0.4 N (0.1 lb) to 35.6 kN (8000 lb), respectively, at tow speeds of 5.15 and 15.46 m/s (10 and 30 knots). All of the depressor configurations selected for this analysis had a lift-to-drag ratio of 4.7 (ϕ = 78 degrees) with variations of the depressor configuration only consisting of changes to the magnitude of the tension force. The values of C_R and C_S were determined using the mathematical expressions presented above for tow speeds of 5.15 and 15.46 m/s (10 and 30 knots).

RESULTS

The results of the calculations for tow speeds of 5.15 and 15.46 m/s (10 and 30 knots) are shown graphically in Figures A.1 and A.2, respectively. Both of these figures present the kite angle at the towing platform as a function of depressor force for selected scope lengths.

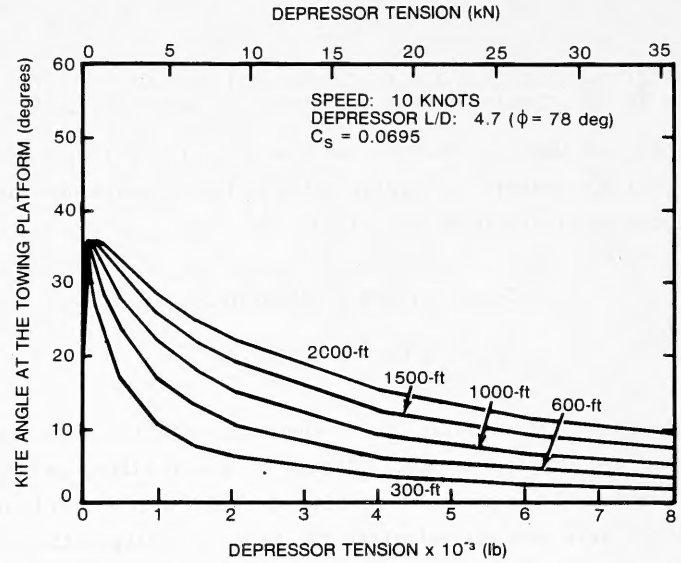

Figure A.1 - Kite Angle as a Function of Depressor Tension at Selected Towline Scopes at 5.15 m/s (10 Knots)

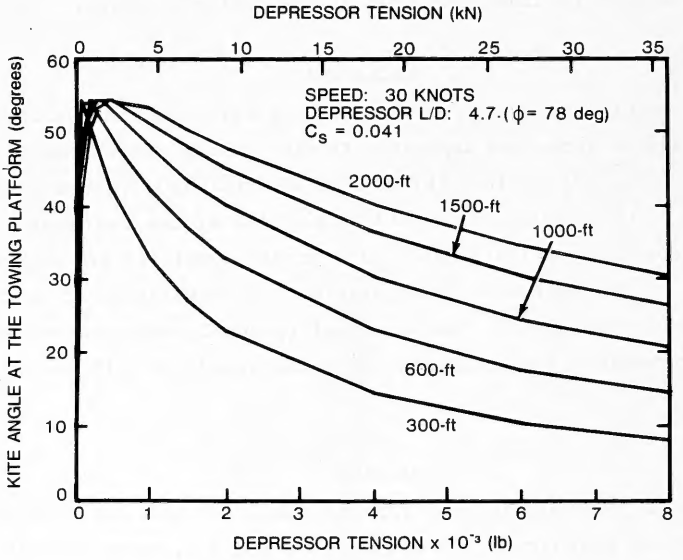

Figure A.2 - Kite Angle as a Function of Depressor Tension at Selected Towline Scopes at 15.46 m/s (30 Knots)

DTNSRDC ISSUES THREE TYPES OF REPORTS

1. DTNSRDC REPORTS, A FORMAL SERIES, CONTAIN INFORMATION OF PERMANENT TECHNICAL VALUE. THEY CARRY A CONSECUTIVE NUMERICAL IDENTIFICATION REGARDLESS OF THEIR CLASSIFICATION OR THE ORIGINATING DEPARTMENT.

2. DEPARTMENTAL REPORTS, A SEMIFORMAL SERIES, CONTAIN INFORMATION OF A PRELIMINARY, TEMPORARY, OR PROPRIETARY NATURE OR OF LIMITED INTEREST OR SIGNIFICANCE. THEY CARRY A DEPARTMENTAL ALPHANUMERICAL IDENTIFICATION.

3. TECHNICAL MEMORANDA, AN INFORMAL SERIES, CONTAIN TECHNICAL DOCUMENTATION OF LIMITED USE AND INTEREST. THEY ARE PRIMARILY WORKING PAPERS INTENDED FOR INTERNAL USE. THEY CARRY AN IDENTIFYING NUMBER WHICH INDICATES THEIR TYPE AND THE NUMERICAL CODE OF THE ORIGINATING DEPARTMENT. ANY DISTRIBUTION OUTSIDE DTNSRDC MUST BE APPROVED BY THE HEAD OF THE ORIGINATING DEPARTMENT ON A CASE-BY-CASE BASIS.